OPEN ACCESS

LINC01094 promotes human nasal epithelial cell epithelial-to-mesenchymal transition and pyroptosis via upregulating HMGB1*

Zizhen Liu#, Yifei Fu#, Wei Huang, Changwu Li, Xin Wei, Jiabin Zhan, Jing Zheng

Department of Otorhinolaryngology Head and Neck Surgery, Hainan General Hospital, Hainan Affiliated Hospital of Hainan Medical University, Haikou, Hainan Province, P.R. China

Rhinology 62: 1, 88 - 100, 2024
https://doi.org/10.4193/Rhin23.184

***Received for publication:**
May 26, 2023
Accepted: September 28, 2023

shared first authors

Abstract

Background: Excessive epithelial-to-mesenchymal transition (EMT) of nasal epithelial cells (NECs) play a prominent role in chronic rhinosinusitis with nasal polyps (CRSwNP) pathogenesis. Long intergenic non-coding RNA 01094 (LINC01094) was previously reported to be overexpressed in CRSwNP, while the regulatory mechanism by which LINC01094 regulates CRSwNP progression remains unclear. Our study aimed to investigate the role of LINC01094 in CRSwNP development.

Methods: hNEC were isolated from tissues of controls and CRSwNP patients and stimulated with interleukin (IL)-13. 3-(4, 5-Dimethylthiazolyl2)-2, 5-diphenyltetrazolium bromide (MTT) assay was employed to analyze hNEC viability. Flow cytometry was employed to analyze pyroptosis. Immunofluorescence was employed to analyze Snail nuclear translocation. The interactions between LINC01094, fused in sarcoma (FUS) and high mobility group box-1 (HMGB1) were analyzed by RNA immunoprecipitation (RIP) and RNA pull-down assays.

Results: LINC01094 and EMT-related proteins were markedly upregulated in nasal polyp tissues of CRSwNP. LINC01094 knockdown inhibited IL-13-induced hNEC EMT and pyroptosis. LINC01094 promoted HMGB1 expression in CRSwNP by binding with FUS. HMGB1 promoted Snail nuclear import in GSK-3β phosphorylation-dependent manner.

Conclusion: LINC01094 facilitated hNEC EMT and pyroptosis in CRSwNP by activating the HMGB1/GSK-3β/Snail axis, which suggested that LINC01094 might serve as a biomarker and therapeutic target in CRSwNP.

Key words: CRSwNP, nasal epithelial cell, epithelial-to-mesenchymal transition, pyroptosis, LINC01094

Introduction

Chronic rhinosinusitis with nasal polyps (CRSwNP) is a common heterogeneous sinus inflammatory disease characterized by exaggerated type 2 response [1]. The incidence of CRSwNP is increasing year by year [2]. Surgical intervention is currently the main treatment strategy for CRSwNP, but the recurrence rate after surgery is as high as 40% to 60% [3]. Therefore, it is urgent to develop novel therapeutic strategies targeting CRSwNP, and understanding the pathogenesis of CRSwNP is the most important step to achieve the goal.

Excessive pyroptosis and epithelial-to-mesenchymal transition (EMT) of nasal epithelial cells (NECs) is closely related to CRSwNP pathogenesis [4, 5]. As reported, EMT is widely present in the nasal mucosa of CRSwNP patients and contributes to the pathogenesis of the disease by promoting the tissue remodeling of nasal polyps [6, 7]. Meanwhile, it was previously described that elevated pyroptosis in NECs contributes to glucocorticoid resistance by affecting glucocorticoid receptor homeostasis in patients with CRSwNP [5]. Therefore, inhibiting EMT of NEC might be a potential therapeutic strategy for CRSwNP. Long non-coding RNAs (LncRNAs) are non-coding RNA molecules with a length of about 200 nts, which are involved in various biological processes[8].

Notably, it's observed that lncRNA dysregulation facilitates CRSwNP development [9]. Exploring the roles of lncRNAs in CRSwNP progression provide insights for its diagnosis and treatment. As a recent research hotspot, long intergenic non-coding RNA 01094 (LINC01094) is identified as an oncogene in multiple malignancies [10, 11]. As widely reported, LINC01094 is correlated with EMT during the progression of cancer [10, 12, 13]. LINC01094 was reported to be upregulated in CRSwNP [9], suggesting that LINC01094 might be related to CRSwNP development. Nevertheless, the molecular mechanism of LINC01094 in regulating CRSwNP progression by affecting EMT and pyroptosis remains unclear.

Subsequently, the downstream regulatory mechanism of LINC01094 in CRSwNP progression was investigated. As widely illustrated, lncRNAs achieve its role in diseases by regulating downstream targets through binding with RNA-binding proteins (RBPs) [14]. As proof, lncRNA GAS6-AS1 promoted tumorigenesis and metastasis of colorectal cancer by regulating TRIM14 through binding to RBP fused in sarcoma (FUS) [15]. In addition, LINC01094 reduced PTEN expression by antagonizing the function of AZGP1 to facilitate gastric cancer cell proliferation and metastasis [16]. Therefore, it's preliminarily speculated that LINC01094 might play a role in CRSwNP by regulating downstream genes through interacting with RBP. High mobility group box-1 (HMGB1), a highly conserved nucleoprotein [17], exacerbates inflammatory diseases by activating cell pyroptosis [18]. Specifically, it was reported that HMGB1 was highly expressed in CRSwNP [19], and HMGB1 translocation from nucleus to cytoplasm in NECs contributed to CRSwNP development [20]. All these pieces of evidence suggest that HMGB1 is related to CRSwNP development. However, it's unclear whether there is a regulatory relationship between LINC01094 and HMGB1. Herein, it was found that FUS was an RBP common to LINC01094 and HMGB1 using bioinformatics prediction, revealing a potential regulatory relationship between LINC01094 and HMGB1. However, there are currently no literature reports on the interaction between LINC01094 and HMGB1 in CRSwNP progression, which deserves further research. Moreover, the glycogen synthase kinase (GSK)-3β/Snail signaling pathway, as the classical downstream pathway of serine/threonine kinase (AKT), functions as the downstream pathway of HMGB1 in promoting prostate cancer cell EMT [21]. However, it remains unclear that the GSK-3β/Snail signaling pathway acts as a key mechanism in regulating hNEC pyroptosis and EMT during CRSwNP progression by HMGB1. Based on the above evidence, it's speculated that LINC01094 promotes HMGB1 expression through binding with FUS to activate the GSK-3β/Snail pathway, thereby facilitating hNEC EMT and pyroptosis to accelerate CRSwNP progression. Our research reveals that LINC01094 may act as a molecular target for treatment strategies for CRSwNP.

Materials and methods

Clinical samples collection

The inferior turbinate mucosa tissues and nasal polyp tissues were collected form controls (n=20) and CRSwNP patients, respectively, in the Hainan General Hospital, Hainan Affiliated Hospital of Hainan Medical University. Chronic rhinosinusitis is divided into CRSwNP and CRS without nasal polyps (CRSsNP). The sinus mucosa tissues were collected form diagnosed CRSsNP patients (n=8) undergoing functional endoscopic sinus surgery for CRSsNP performed. The CRSwNP group involved patients diagnosed with CRSwNP undergoing functional endoscopic sinus surgery for CRSwNP performed. CRSwNP and CRSsNP were diagnosed according to the current Ameriacan guideline and the European Position Paper on Rhinosinusitis and Nasal Polyps 2020 [22]. CRSwNP can be divided into eosinophilic CRSwNP (eCRSwNP) subtype and noneosinophilic CRSwNP (neCRSwNP) subtype [23]. Among the 20 samples we collected, 11 were eCRSwNP and 9 were neCRSwNP. Patients with other serious medical conditions, such as autoimmune dysfunction and malignant tumors, were not included in this study. The control group consisted of simple deviated septum or simple sinus cyst, trauma patients undergoing septoplasty, conchoplasty or rhinoplasty, without a history of chronic or acute rhinosinusitis. All tissues were cryopreserved at -80°C. This study passed the review of Ethics Committee of Hainan General Hospital, Hainan Affiliated Hospital of Hainan Medical University Hospital before enrollment of patients and all participants signed informed consent.

Cell culture and treatment

The tissues were cut into $1mm^3$, digested in dispase II and trypsin (Sigma-Aldrich). hNECs were obtained by filtration with a 100 μm cell strainer. Cells were culured in complete DMEM (Gibco, MD, USA) for 30 min to remove fibroblasts. hNECs were cultured by using an air-liquid interface (ALI) method as previously described [24]. In brief, hNECs were seeded at passage 2–3 at a density of 1×10^5 cells/cm^2 on Transwell inserts (Transwell, 12 wells, 0.4 μm, Corning, NY, USA) in complete DMEM and differentiated with PneumaCult-ALI Medium (STEMCELL Technologies). A successfully differentiated ALI culture contains basal cells, tight junctions, secretory cells (primarily mucus-secreting goblet cells) and ciliated epithelial cells. For IL-13 treatment, hNEC were treated with different concentrations (1, 5, 10 and 20 ng/mL) recombinant human IL-13 (STEMCELL, Vancouver, BC, Canada) for 12, 24, 36 and 48 h as previously reported [25].

Cell transfection

The short hairpin RNA of LINC01094 (si-LINC01094-1 and si-LINC01094-2), the overexpression plasmid of FUS (Oe-FUS), the small interfering RNA of Snail (si-Snail) and their negative controls, were purchased from GenePharma (Shanghai, China).

Before transfection, 1×10^6 hNECs were cultured in 6-well plates with 2 mL complete medium for 24 h until they were 90% confluent. Then hNECs were transfected with the above plasmids (50 ng) with Lipofectamine™ 3000 (Invitrogen, CA, USA). After 48 h, fluorescent expression was observed and photographed using a fluorescent microscope (Olympus). Thereafter, samples were collected, and the transfection efficiency was identified using qRT-PCR.

3-(4, 5-Dimethylthiazolyl2)-2, 5-diphenyltetrazolium bromide (MTT) assay

hNEC were cultured in 96-well plates (2×103 cells/well) for 24 h and incubated with 20 µL MTT (5 mg/mL, Beyotime, Shanghai, China) for 4 h at 37°C. The precipitate was dissolved in dimethyl sulfoxide (DMSO, 100 µL, Sigma-Aldrich, MO, USA), and the absorbance at 490 nm was subsequently analyzed with a spectrometer (Bioteke, Beijing, China).

Detection of pyroptosis by flow cytometry

hNEC were cultured in 24-well plates (2×10^4 cells/well) for 24 h and subsequently stained with FITC-caspase-1 and PI using the FLICA 660 caspase-1 assay kit (Immunochemistry, MN, USA) and PI kit (Beyotime). Cells were then analyzed using a FACS Calibur (BD). A gating strategy is shown (FSC vs SSC, Live/death marker and singlets) in Figure S3.

Immunofluorescence

Cells were seeded on glass coverslips. After incubation in 100% methanol (chilled at −20 °C) at room temperature for 5 min, cells were washed three times with ice-cold PBS. Next, cells were incubated with 1% BSA for 30 min and then with antibodies against Snail (Abcam, 5 µg/mL, ab224731), followed by incubation with the corresponding secondary antibody (Abcam, 1:3000, ab7148) for 1 h at room temperature in the dark. Finally, the nucleus was stained with DAPI (Sangon, Shanghai, China), and cells were sealed with the sealing liquid. The images were collected with a fluorescence microscope (Olympus). The experiment was repeated three times, and five fields were randomly selected to analyze the fluorescence intensity using Image-J software.

RNA pull-down assay

Biotin-labelled LINC01094 was in vitro transcribed with HiScribe™ T7 Quick High Yield RNA Synthesis Kit (NEB, Beijing, China) with Biotin-16-UTP (Roche, Basel, Switzerland), treated with RNase-free DNase I on column during RNA purification with RNA Clean & Concentrator-25 (Zymo Research, CA, USA). For each sample, 5 µg RNA was mixed with 1×10^7 cell extract and incubated at 4 °C for 1 h, followed by incubating with Dynabeads M-280 Streptavidin (Invitrogen) at 4 °C overnight. After washes, the pull-down complexes were eluted by denaturation in 1× protein loading buffer for 10 min at 100 °C. The samples were detected by western blot analysis.

RNA immunoprecipitation (RIP) assay

RIP assay was performed using the Magna RIPTM RBP Immunoprecipitation Kit (No.17-700, Millipore, MA, USA) Cells were lysed with a complete RIP lysis buffer. Cell extract was incubated with IgG (Abcam, Cambridge, UK, 1:50, ab172730) and FUS (Abcam, 1:50, ab243880) antibodies at 4°C overnight. The recovered RNA-protein complex was washed six times with wash buffer and protein denaturation at 55°C. The cDNA was synthesized and subjected to qRT-PCR assay.

Quantitative real-time polymerase chain reaction (qRT-PCR)

Total RNA was extracted from nasal polyp tissues and hNEC with TRIzol (ThermoFisher Scientific, MA, USA). The quantity of RNA was determined using a NanoDrop 2000 spectrophotometer (Thermo Scientific, MA, USA). The 260/280 nm absorbance ratio was 1.9-2.1, demonstrating a good degree of purity. The cDNA was synthesized using the Reverse Transcription Kit (Toyobo, Tokyo, Japan) and subjected to qRT-PCR assay with SYBR (ThermoFisher Scientific). GAPDH was used as the reference gene for mRNA. The data was analyzed with $2-\Delta\Delta CT$ method. The primers were listed as follows (5′-3′): LINC01094 (F): TGTAAAACGACGGCCAGT, LINC01094 (R): CAGGAAACAGCTATGACC; HMGB1 (F): ATATGGCAAAAGCGGACAAG, HMGB1 (R): GCAACATCACCAATGGACAG; GAPDH (F): CCAGGTGGTCTCCTCTGA, GAPDH (R): GCTGTAGCCAAATCGTTGT.

Western blot

The proteins were isolated from nasal polyp tissues and hNEC with RIPA and quantified by a BCA kit (Beyotime). Subsequently, total protein (20 µg) was isolated by 10% SDS-PAGE and transferred to a PVDF membrane (Millipore). Then, membranes were blocked and incubated overnight with antibodies against against E-cadherin (Abcam, 1:10000, ab40772), ZO-1 (Abcam, 1:1000, ab276131), vimentin (Abcam, 1:1000, ab92547), Snail (Abcam, 1:1000, ab216347), NLRP3 (Abcam, 1:1000, ab263899), caspase-1 (Abcam, 1:1000, ab207802), GSDMD-N (Abcam, 1:1000, ab215203), FUS (Abcam, 1:1000, ab124923), HMGB1 (Abcam, 1 µg/ml, ab18256), p-GSK-3β (Cell Signaling Technology, CA, USA, 1:1000, #5558), GSK-3β (Abcam, 1:1000, ab93926) and GAPDH antibody (Abcam, 1:10000, ab8245). After washed with PBS-T, membranes were then incubated with secondary antibody (Abcam, 1:10000, ab7090) for 60 min. The membranes were visualized and imaged by GEL imaging system (Bio-Rad, CA, USA). The bands were quantified by Image J (National Institutes of Health, MD, USA).

Statistical analysis

All data were obtained from three independent experiments. Statistical data was analyzed by SPSS 19.0 (IBM, NY, USA) and

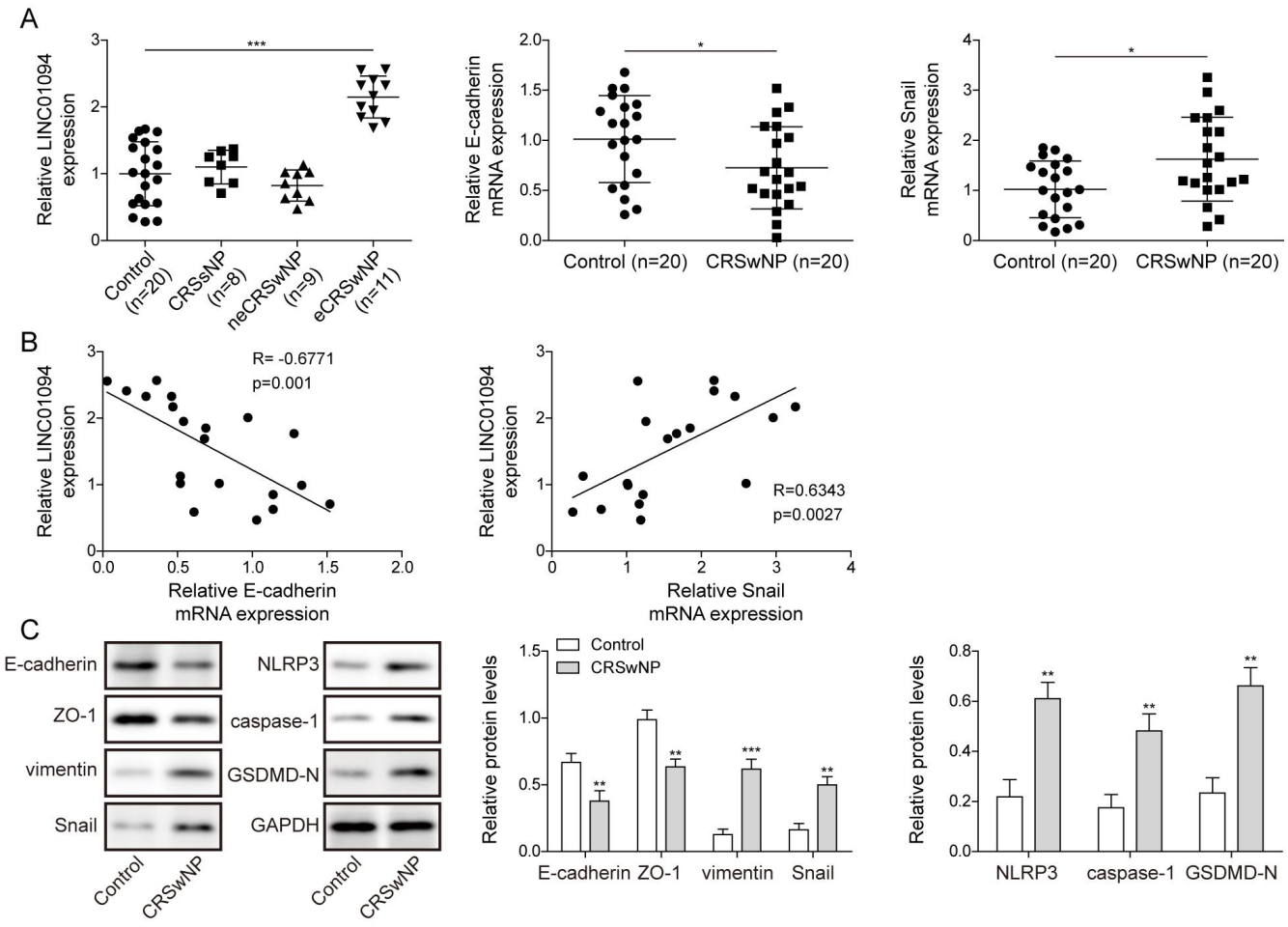

Figure 1. LINC01094 and EMT-related proteins were upregulated in CRSwNP patients.

The inferior turbinate mucosa tissues and nasal polyp tissues were collected from controls (n=20), CRSwNP patients (n=20, including 9 eCRSwNP cases and 11 neCRSwNP cases) and CRSsNP patients (n=8). (A) LINC01094 and EMT-related proteins (Snail and E-cadherin) mRNA levels in tissues were assessed using qRT-PCR. (B) Correlation analysis was employed to analyze the correlation of LINC01094 expression, E-cadherin expression and Snail expression. (C) Western blot was performed to examine EMT-related proteins (vimentin, Snail, E-cadherin, ZO-1) and pyroptosis-related proteins (NLRP3, caspase-1 and GSDMD-N) levels in tissues. N=20. Data were expressed as mean ± SD. n=20. *p< 0.05, **p< 0.01, ***p< 0.001.

expressed as means ± SD. The differences among two groups were analyzed by Student's t-tests. One-way ANOVA followed by Tukey's post hoc test was performed to assess the differences among multiple groups. The p values less than 0.05 were considered significant.

Results

LINC01094 and EMT-related proteins were upregulated in CRSwNP patients

As previously described, LINC01094 was overexpressed in CRSWNP [9]. To investigate the role of LINC01094 in CRSwNP, the inferior turbinate mucosa tissues and nasal polyp tissues were collected from controls, CRSwNP (eCRSwNP and neCRSwNP) patients and CRSsNP patients. As revealed in Figure 1A, the expression of LINC01094 in eCRSwNP was significantly upregulated (fold change: 2.15), which was consistent with the previous report [9], while the expression of LINC01094 in CRSsNP was slightly upregulated without statistical difference (fold change: 1.10). EMT is widely present in the nasal mucosa of CRSwNP patients and contributes to the pathogenesis of the disease [6]. Our results showed that mesenchymal marker (Snail) was upregulated (fold change: 1.59) and epithelial cell marker (E-cadherin) was downregulated (fold change: 0.71) in CRSwNP patients compared to those in the control group, which was consistent with the previous report [26] (Figure 1A). In addition, it was found that LINC01094 expression was negatively correlated with E-cadherin expression (R=0.6771, p=0.001), while its expression was positively correlated with Snail expression (R=0.6343, p=0.0027) (Figure 1B). Meanwhile, the mesenchymal markers (vimentin (fold change: 4.84) and Snail (fold change: 3.06)) as well as pyroptosis-related proteins (NLRP3 (fold change: 2.80), caspase-1 (fold change: 2.75) and GSDMD-N (fold change:

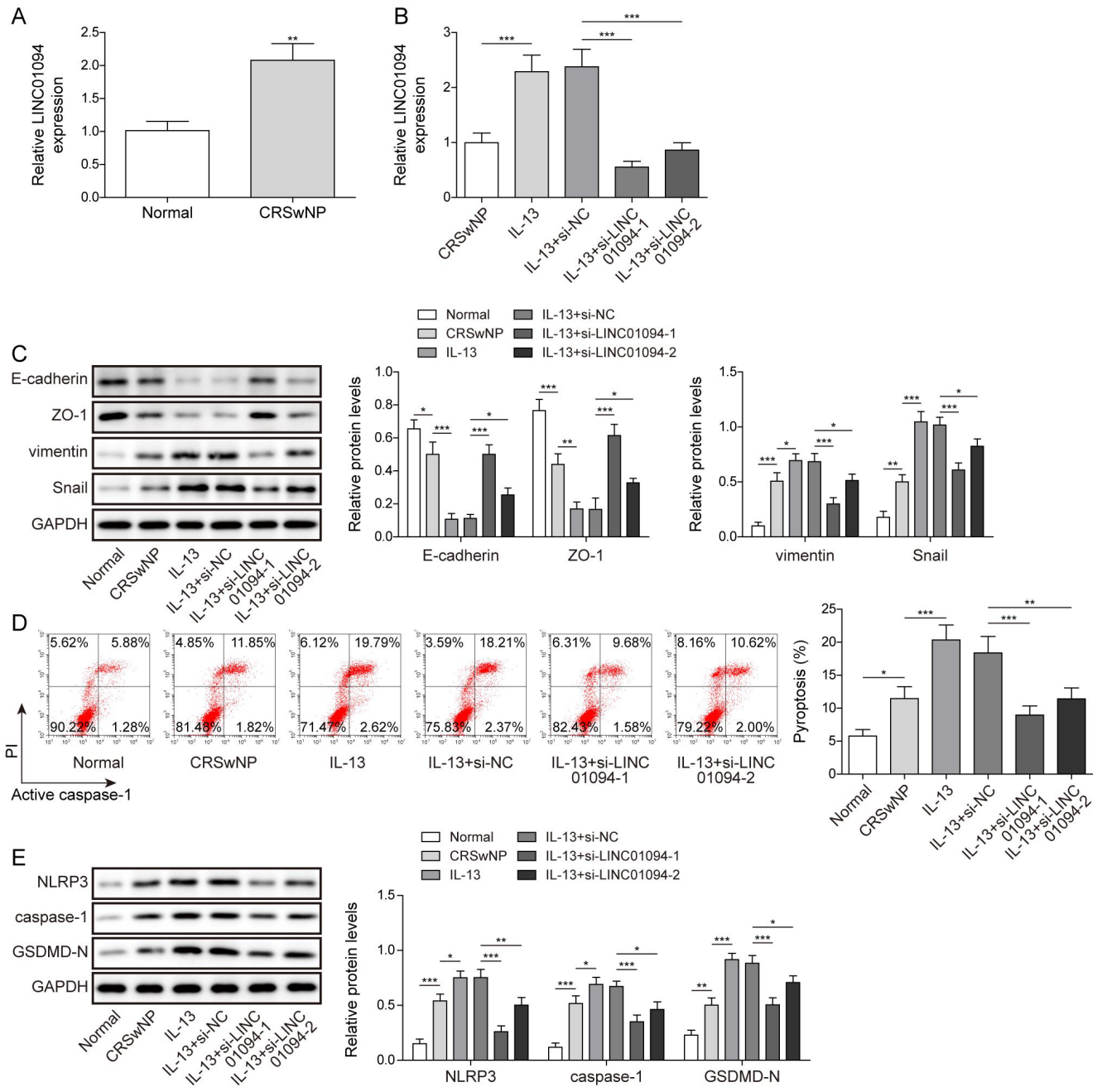

Figure 2. LINC01094 knockdown inhibited IL-13-induced hNEC EMT and pyroptosis.

(A) qRT-PCR was performed to determine LINC01094 expression in hNEC isolated from tissues of controls and CRSwNP patients. CRSwNP patients-derived hNEC were transfected with si-NC or si-LINC01094 and subsequently subjected to IL-13 stimulation. (B) LINC01094 expression in cells was detected by qRT-PCR. (C) EMT-related proteins (vimentin, Snail, E-cadherin, ZO-1) levels were determined by western blot. (D) Flow cytometry was conducted to analyze pyroptosis. (E) Western blot was performed to analyze pyroptosis-related proteins (NLRP3, caspase-1 and GSDMD-N) levels in cells. Data were expressed as mean ± SD. All our data were obtained from three independent experiments. *p< 0.05, **p< 0.01, ***p< 0.001.

2.84)) were significantly upregulated in nasal polyp tissues of CRSwNP patients in comparison with those in tissues of controls, whereas epithelial cell markers (E-cadherin (fold change: 0.57) and ZO-1 (fold change: 0.64)) were downregulated (Figure 1C). Collectively, LINC01094, EMT and pyroptosis might be related to CRSwNP progression.

LINC01094 knockdown inhibited IL-13-induced hNEC EMT and pyroptosis

Subsequently, we further explored the role of LINC01094 in CRSwNP progression at the cellular level. NECs are the first physical barrier of the nasal cavity and are crucial in the occurrence and development of CRSwNP [27]. hNECs were isolated from

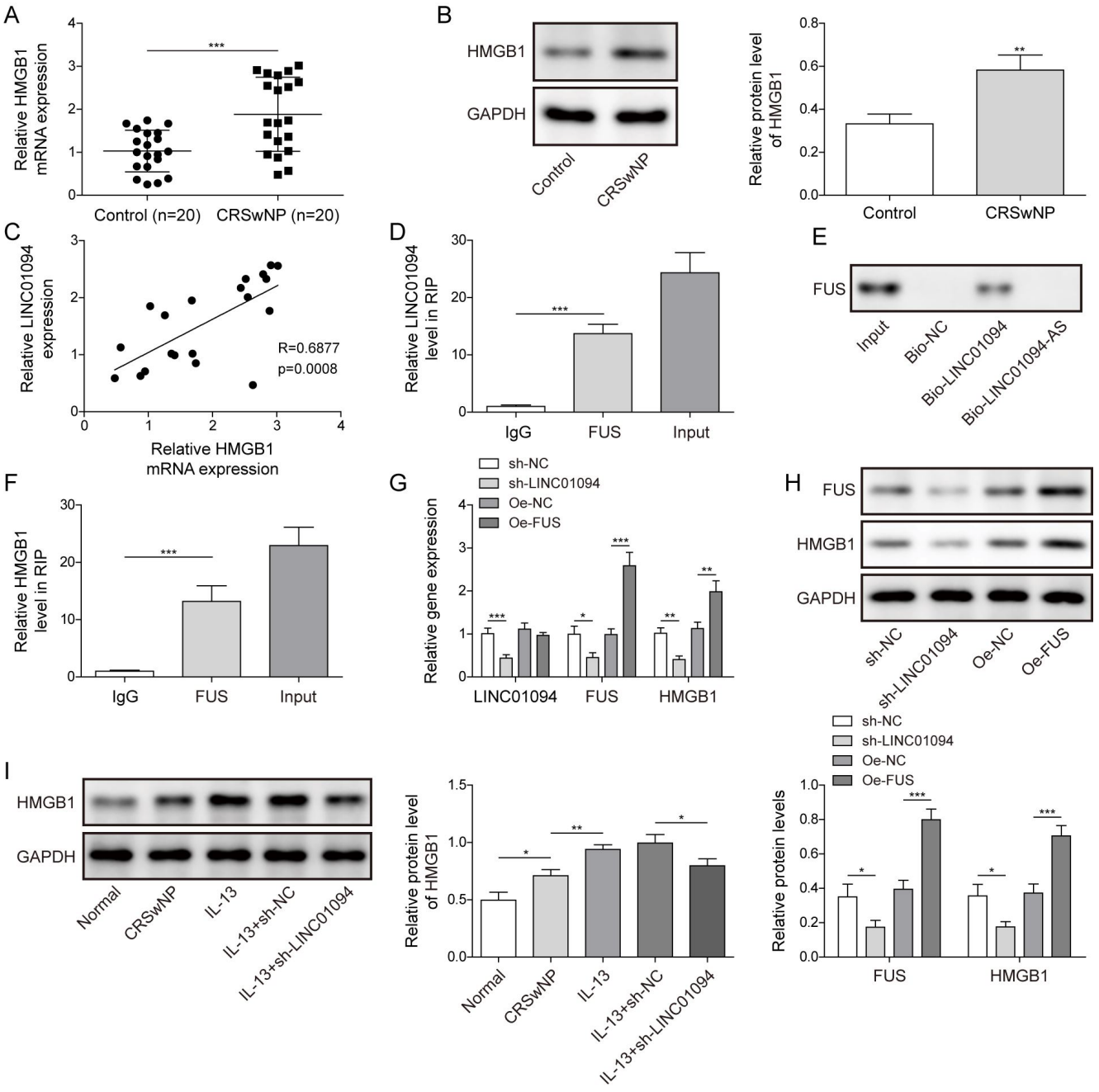

Figure 3. LINC01094 regulated HMGB1 expression via FUS.

(A-B) HMGB1 expression in nasal polyp tissues of CRSwNP patients and inferior turbinate mucosa tissues of controls was assessed using qRT-PCR and western blot. (C) Correlation analysis was employed to analyze the correlation of LINC01094 expression and HMGB1 expression. (D-E) The interaction between LINC01094 and FUS was analyzed by RIP and RNA pull-down assays. (F) RIP assay was conducted to analyze the interaction between FUS and HMGB1. (G-H) LINC01094, FUS and HMGB1 expression levels in CRSwNP patients-derived hNEC were assessed using qRT-PCR and western blot. (I) HMGB1 protein level in cells was evaluated by western blot. Data were expressed as mean ± SD. All our data were obtained from three independent experiments. *p< 0.05, **p< 0.01, ***p< 0.001.

tissues of controls and CRSwNP patients, and it was observed that LINC01094 was significantly upregulated in CRSwNP patients-derived hNECs (fold change: 2.05) (Figure 2A). CRSwNP is a chronic disease of the upper respiratory tract induced by T2 type inflammation, and IL-13 is one of the key factors inducing and maintaining Th2 type inflammation [28]. IL-13-stimulated NECs can mimic CRSwNP in vitro [29]. Herein, hNECs were treated with different concentrations of IL-13 (1, 5, 10 and 20 ng/mL), and it was observed that cell viability was gradually increased by IL-13 stimulation concentration-dependently, with a significant

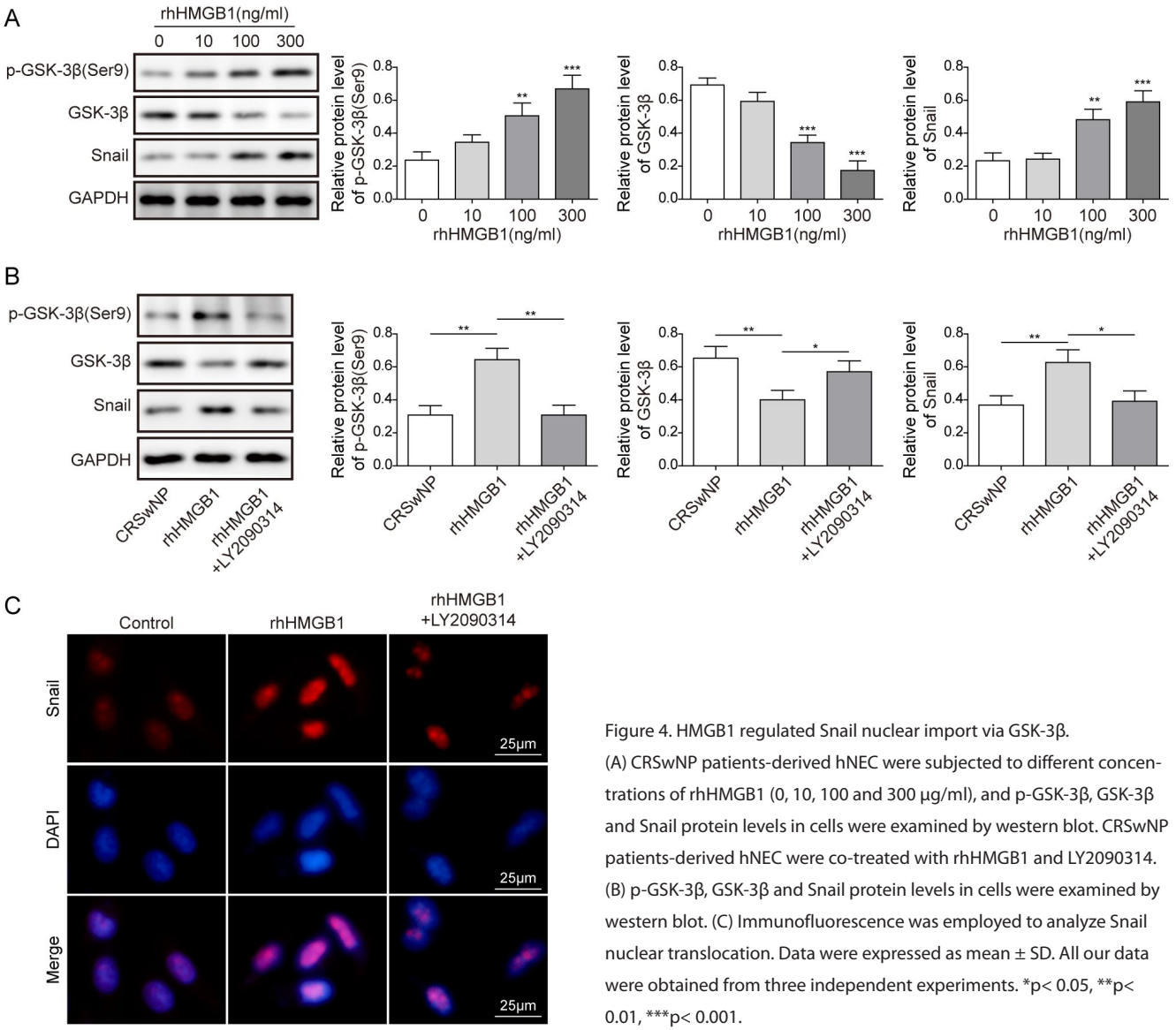

Figure 4. HMGB1 regulated Snail nuclear import via GSK-3β. (A) CRSwNP patients-derived hNEC were subjected to different concentrations of rhHMGB1 (0, 10, 100 and 300 μg/ml), and p-GSK-3β, GSK-3β and Snail protein levels in cells were examined by western blot. CRSwNP patients-derived hNEC were co-treated with rhHMGB1 and LY2090314. (B) p-GSK-3β, GSK-3β and Snail protein levels in cells were examined by western blot. (C) Immunofluorescence was employed to analyze Snail nuclear translocation. Data were expressed as mean ± SD. All our data were obtained from three independent experiments. *p< 0.05, **p< 0.01, ***p< 0.001.

change observed at 10 ng/ml (Figure S1A). Therefore, this concentration (10 ng/ml) was selected for subsequent experiments. As shown in Figure S1B, the fluorescence infection rate was about 80% in hNECs cells after transfected with si-LINC01094-1, si-LINC01094-2 or si-NC. In addition, a significantly reduced expression of LINC01094 was observed in hNECs transfected with si-LINC01094-1 (fold change: 0.27) and si-LINC01094-2 (fold change: 0.51) than those transfected with si-NC, indicating a successful construction of hNECs with LINC01094 knockdown (Figure S1C). LINC01094 expression in CRSwNP patients-derived hNECs was markedly increased after IL-13 treatment (fold change: 2.30), which was reversed by sh-LINC01094-1 and sh-LINC01094-2 (fold change: 0.23 and 0.36) (Figure 2B). As reported, the promotion of NEC proliferation is associated with CRSwNP progression [30]. Consistent with this, we also found that CRSwNP patients-derived hNECs showed stronger cell viability (fold change: 1.527) compared with control-derived hNECs, and IL-13 treatment further facilitated CRSwNP patients-derived hNECviability (fold change: 1.34), while these effects of IL-13 were reversed by LINC01094 knockdown (fold change: 0.62 and 0.77) (Figure S2A). Meanwhile, it was found that epithelial cell markers (E-cadherin (fold change: 0.76) and ZO-1 (fold change: 0.57)) were decreased, and mesenchymal markers (vimentin (fold change: 5.12) and Snail (fold change: 2.80)) were elevated in CRSwNP patients-derived hNECs compared with those in control-derived hNECs, the above results were further enhanced following IL-13 treatment, whereas these effects of IL-13 were eliminated following LINC01094 downregulation (Figure 2C). Pyroptosis is closely related to inflammation and is considered as a key player in promoting CRSwNP progression (5). Consistent with this, increased expressions of pyroptosis-related proteins (NLRP3 (fold change: 3.59), caspase-1 (fold change: 4.34) and GSDMD-N (fold change: 2.19)) and increased pyroptosis (fold change: 1.98) were observed in CRSwNP patients-derived hNECs

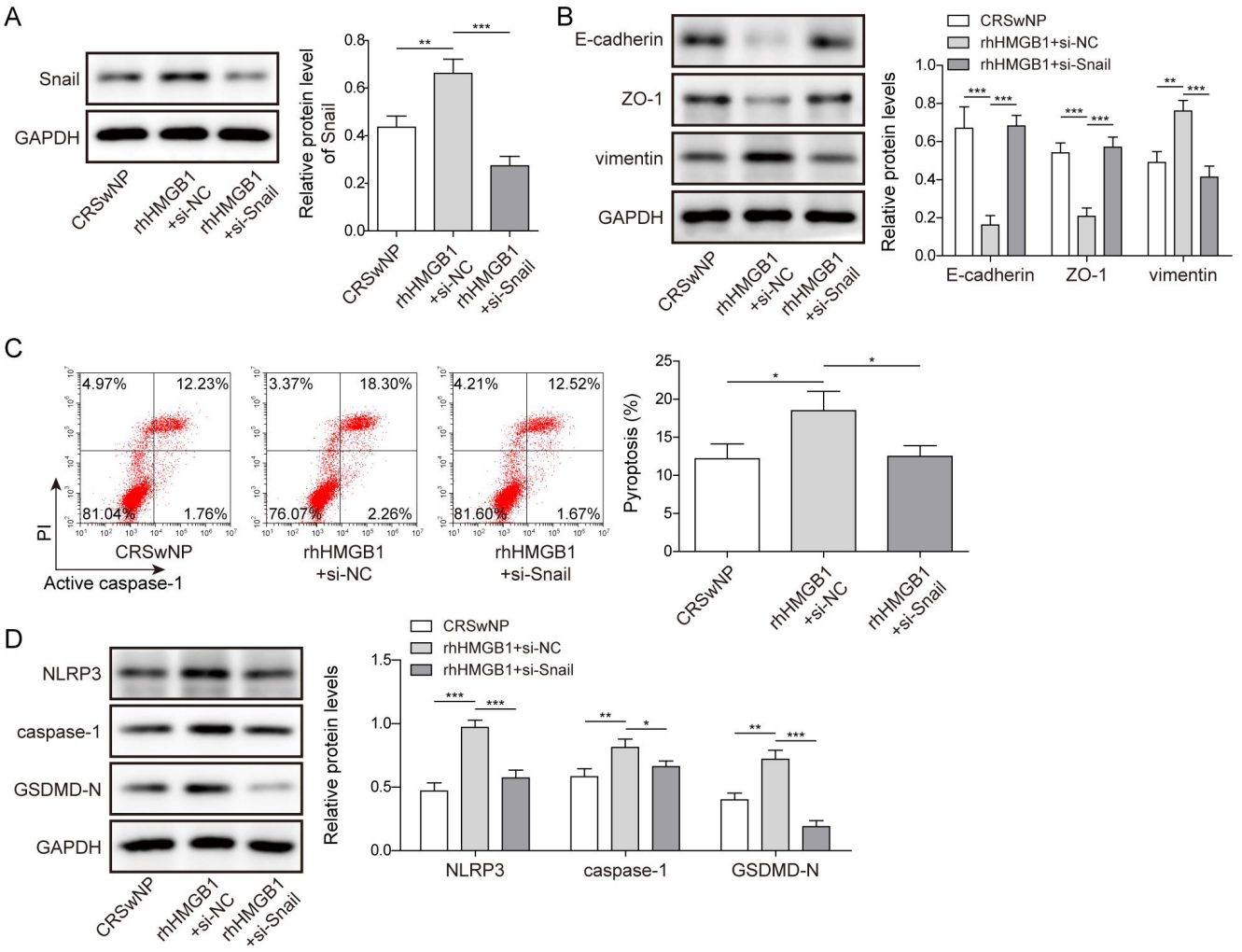

Figure 5. HMGB1 promoted hNEC EMT and pyroptosis by activating the GSK-3β/Snail pathway.

CRSwNP patients-derived hNEC were treated with rhHMGB1 and transfected with si-Snail meanwhile. (A) Western blot was carried out to analyze Snail protein level in cells. (B) Western blot was employed to examine EMT-related proteins (vimentin, Snail, E-cadherin, ZO-1) levels in cells. (C) Flow cytometry was employed to analyze pyroptosis. (D) Pyroptosis-related proteins (NLRP3, caspase-1 and GSDMD-N) levels in cells were determined using western blot. Data were expressed as mean ± SD. All our data were obtained from three independent experiments. *p< 0.05, **p< 0.01, ***p< 0.001.

compared with control-derived hNECs, and IL-13 treatment further enhanced the trend, while this effect of IL-13 was abrogated by LINC01094 silencing (Figure 2D-E). Collectively, LINC01094 knockdown inhibited IL-13-induced hNEC EMT and pyroptosis.

LINC01094 regulated HMGB1 expression via FUS

Next, we further explored the regulatory mechanism of LINC01094 in CRSwNP. HMGB1 is highly expressed in CRSwNP and contributes to inflammatory responses in this disease [19]. Consistent with this, our results also showed that HMGB1 was upregulated in CRSwNP patient nasal polyp tissue (fold change: 1.82 and 1.75) (Figure 3A-B). It also turned out that LINC01094 expression was positively correlated with HMGB1 expression in CRSwNP patients (R=0.6877, p=0.0008) (Figure 3C). We subsequently found that LINC01094 directly bound with FUS (fold change: 13.57) (Figure 3D-E). Interestingly, as revealed in Figure 3F, HMGB1 also bound to FUS (fold change: 13.15). Moreover, LINC01094 (fold change: 0.44), FUS (fold change: 0.45) and HMGB1 (fold change:0.39) expression levels in CRSwNP patients-derived hNEC were reduced after LINC01094 knockdown, while FUS overexpression resulted in unchanged LINC01094 expression and increased FUS (fold change: 2.63) and HMGB1 expressions (fold change: 1.76) (Figure 3G-H). Finally, it was found that HMGB1 was upregulated (fold change: 1.43) in CRSwNP patients-derived hNEC compared with that in control-derived hNEC, and IL-13 treatment further increased HMGB1 expression in cells (fold change: 1.32), whereas this effect of IL-13 was abolished by LINC01094 downregulation (fold change: 0.80) (Figure 3I). Taken together, LINC01094 promoted HMGB1 expression in

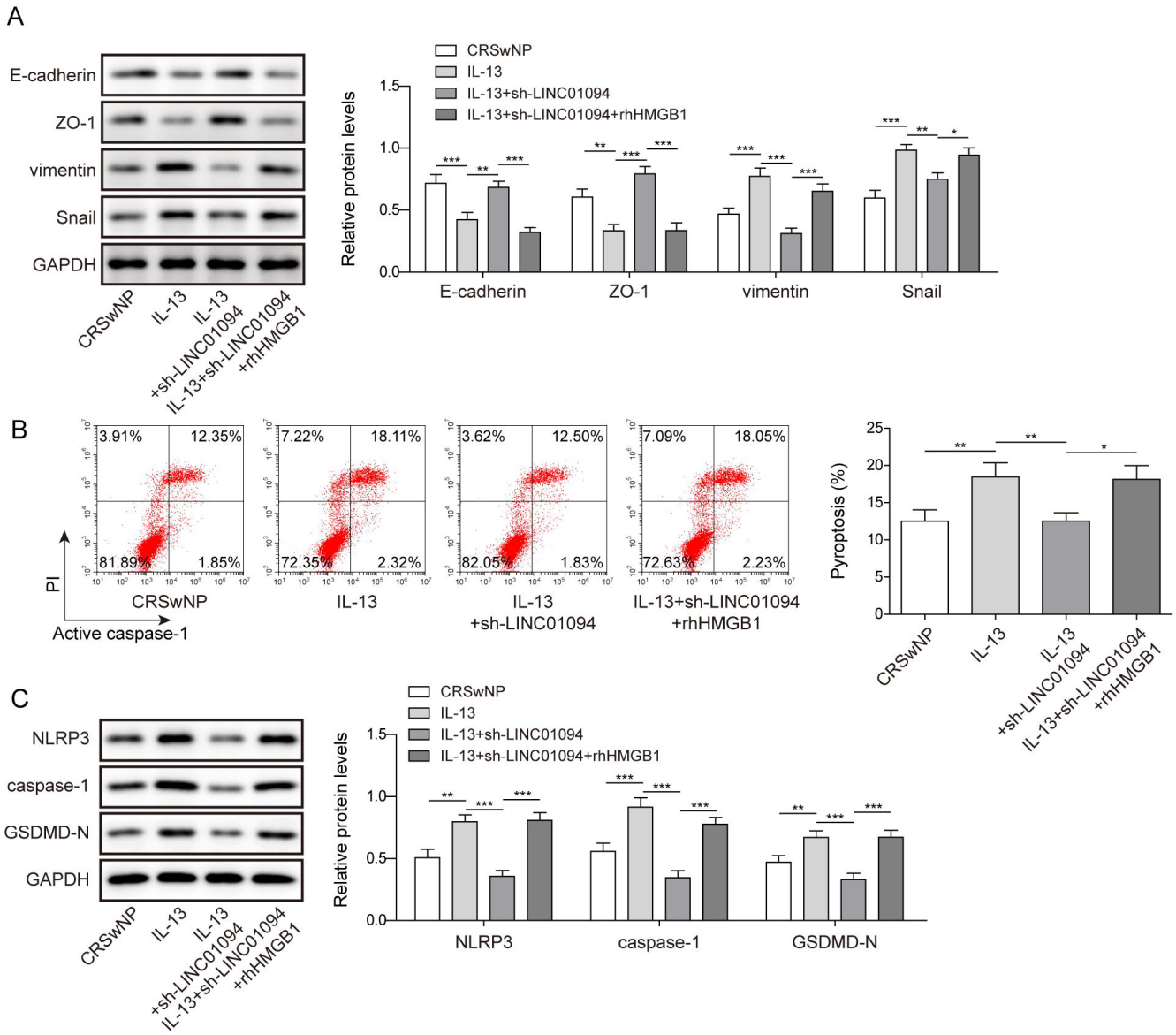

Figure 6. LINC01094 promoted hNEC EMT and pyroptosis by upregulating HMGB1.

CRSwNP patients-derived hNEC were treated with rhHMGB1 and transfected with si-LINC01094 meanwhile. (A) EMT-related proteins (vimentin, Snail, E-cadherin, ZO-1) levels in cells were determined by western blot. (B) Flow cytometry was employed to analyze pyroptosis. (C) Western blot was performed to detect pyroptosis-related proteins (NLRP3, caspase-1 and GSDMD-N) levels in cells. Data were expressed as mean ± SD. All our data were obtained from three independent experiments. *p< 0.05, **p< 0.01, ***p< 0.001.

CRSwNP by binding with FUS.

HMGB1 regulated Snail nuclear import via GSK-3β

The regulatory mechanism of HMGB1 in CRSwNP was subsequently investigated. The GSK-3β/Snail is a classical pathway for activating EMT [31]. Herein, our results revealed that recombinant human HMGB1 (rhHMGB1) treatment could increase p-GSK-3β (fold change: 2.14) and Snail protein levels (fold change: 1.98) and reduce GSK-3β level (fold change: 0.57) in CRSwNP patients-derived hNEC in a dose-dependent manner (Figure 4A). We selected rhHMGB1 at 100 ng/ml concentration for subsequent experiments. As shown in Figure 4B, rhHMGB1 increased p-GSK-3β (fold change: 2.09) and Snail (fold change: 1.70) levels and reduced GSK-3β level (fold change: 0.61) in CRSwNP patients-derived hNEC, which was reversed after LY2090314 (GSK-3β inhibitor) treatment. In addition, rhHMGB1 treatment could promoted Snail nuclear import, which was reversed by LY2090314 administration (Figure 4C). In summary, HMGB1 facilitated Snail nuclear import in CRSwNP by activating GSK-3β.

HMGB1 promoted hNEC EMT and pyroptosis by activating the GSK-3β/Snail pathway

To study the role of HMGB1/GSK-3β/Snail axis in regulating CRSwNP development, CRSwNP patients-derived hNEC were treated with rhHMGB1 and transfected with si-Snail meanwhile. It was firstly observed that rhHMGB1 treatment markedly increased Snail level in CRSwNP patients-derived hNEC (fold change: 1.52), while this effect was abolished by si-Snail transfection (fold change: 0.41) (Figure 5A). rhHMGB1 increased CRSwNP patients-derived hNEC viability (fold change: 1.54), which were eliminated by Snail knockdown (fold change: 0.61) (Figure S2B). Additionally, rhHMGB1 treatment reduced E-cadherin (fold change: 0.24) and ZO-1 (fold change: 0.38) protein levels and increased vimentin level (fold change: 1.55) in CRSwNP patients-derived hNEC, while these protein changes were reversed by Snail downregulation (fold change: 4.2, 2.76 and 0.54) (Figure 5B). Moreover, Snail knockdown reversed the promoting effect of rhHMGB1 on pyroptosis (fold change: 0.67) (Figure 5C) and the levels of pyroptosis-related proteins (fold change: 0.59, 0.81 and 0.26) (Figure 5D). In conclusion, HMGB1 facilitated hNEC EMT and pyroptosis by activating the GSK-3β/Snail pathway.

LINC01094 promoted hNEC EMT and pyroptosis by upregulating HMGB1

To uncover the molecular mechanism of LINC01094/HMGB1 axis on hNEC EMT and pyroptosis in CRSwNP, CRSwNP patients-derived hNEC were treated with rhHMGB1 and transfected with si-LINC01094 meanwhile. As shown in Figure S2C, rhHMGB1 treatment abolished LINC01094 downregulation's inhibition effects on IL-13-mediated increase in CRSwNP patients-derived hNEC viability (fold change: 1.54). Moreover, rhHMGB1 treatment ameliorated si-LINC01094-induced increase in E-cadherin (fold change: 0.47) and ZO-1 (fold change: 0.42) protein levels and prevented si-LINC01094-induced decrease in vimentin (fold change: 2.09) and Snail levels (fold change: 1.26) (Figure 6A). Meanwhile, the inhibitory effects of LINC01094 downregulation on pyroptosis (fold change: 1.45) and the levels of pyroptosis-related proteins in IL-13-treated hNEC were restored by rhHMGB1 (fold change: 2.26, 2.25 and 2.03) (Figure 6B-C). In total, LINC01094 achieved its role in promoting hNEC EMT and pyroptosis during CRSwNP development by targeting HMGB1.

Discussion

CRSwNP is a heterogeneous disease involving multiple structural cells, cellular processes and inflammatory mediators [32]. The pathophysiological mechanisms underlying CRSwNP remain unclear. It has been illustrated that EMT activation in NECs accelerates tissue remodeling in CRSwNP patients and exacerbates the disease [4]. It's suggested that understanding the regulatory mechanism of hNEC in EMT can help develop novel therapeutic strategies against CRSwNP. In the current research, we found that LINC01094 facilitated the EMT and pyroptosis of hNEC during CRSwNP progression by activating the HMGB1/GSK-3β/Snail axis.

LncRNAs function in nearly all parts of gene control, including epigenetic developmental control, nuclear-cytoplasmic transport, and transcription and function in regulating various biological processes including cell proliferation, metastasis, invasion, and inflammation [33]. LncRNA dysregulation is a common feature of various inflammatory diseases [34]. Nevertheless, there are few studies on CRSwNP and lncRNAs. LINC01094 is a classic oncogene [11, 35]. Notably, a recent research has revealed that LINC01094 was highly expressed in CRSwNP [9]. Nevertheless, the function of LINC01094 in CRSwNP hasn't been fully clarified. Herein, it was found that LINC01094 was significantly upregulated in nasal polyp tissues of CRSwNP patients (including eCRSwNP and neCRSwNP subtypes) compared to those in tissues of controls, and LINC01094 expression was slightly increased in CRSsNP compared with the control group. As well known, NECs act as key roles in CRSwNP pathogenesis [36]. Several studies have indicated that hNECs can represent human nasal polyps (NPs) and be easily separated from NP tissues [37, 38]. hNECs are also commonly used cells for in vitro research on the pathogenesis of CRSwNP [39]. In the current study, hNECs were isolated from patients diagnosed with CRSwNP according to the current American guideline and the European Position Paper on Rhinosinusitis and Nasal Polyps 2020. Herein, our results showed that LINC01094 was highly expressed in hNEC isolated from tissues of CRSwNP patients and controls. EMT refers to the biological process by which epithelial cells are transformed into cells with a mesenchymal phenotype by a specific program [8]. It has been widely illustrated that EMT activation in NECs accelerates the tissue remodeling of nasal polyps to promote CRSwNP progression [4]. IL-13 is one of the key factors inducing and maintaining Th2 type inflammation [40]. In the present work, we treated hNECs with IL-13 to maintain or worsen the pathological related functions of CRSwNP. Our further experiments demonstrated that LINC01094 knockdown increased epithelial cell markers (E-cadherin and ZO-1) and reduced mesenchymal markers (vimentin and Snail) in IL-13-treated hNECs, suggesting that LINC01094 affected CRSwNP progression by regulating EMT. Moreover, pyroptosis is an inflammatory programmed death caused by the infection of intracellular pathogens. Excessive activation of hNEC pyroptosis is the leading cause of CRSwNP pathogenesis [5]. Herein, our results showed that IL-13 stimulation further promoted pyropotsis in CRSwNP. In addition, LINC01094 knockdown inhibited IL-13-induced hNEC pyroptosis. Moreover, the pathophysiological mechanism of CRSwNP involves a variety of inflammatory cells and complicated inflammatory reaction [41, 42], and CRSwNP is characterized histologically by hyperplastic nasal epithelium and epithelial cell proliferation [43, 44]. As revealed by Deng et al., YAP upregulated NEC proliferation and epithelium-derived inflammatory cytokine expression via NF-κB Pathway in nasal polyps during CRSwNP progression [45]. Remarkably,

the up-regulated epithelial cell proliferation observed in polyps could be induced by IL-6 in the case of prior epithelial damage [46]. That evidence suggested that the enhancement of NEC proliferation plays an important role in the pathogenesis of CRSwNP and is related to inflammation. As previously reported, both cell proliferation and pyropotsis were increased in bone marrow-derived macrophages during atherosclerosis progression, which suggested that inflammasome activation creates a feedforward loop to promote proliferation but also leads to pyroptotic cell death [47]. In addition, epithelial cells undergo rapid proliferation in response to lysophosphatidic acid resulting in a transient decrease in inflammatory cytokines followed by an upregulation of these cytokines that could lead to increased inflammation [48]. In the current study, both abnormal NEC proliferation and uncontrolled NEC inflammation are observed in CRSwNP, which is related to the pathogenesis of CRSwNP. However, the specific relationship between proliferation and inflammation requires further experimental verification in the future. All our results suggested that LINC01094 upregulation in CRSwNP facilitated hNEC EMT and pyroptosis. It is interesting that chronic sinusitis (CRS) is closely related to NPs. CRS is mainly caused by chronic inflammation of the nasal mucosa in patients, which stimulates the nasal mucosa for a long time, leading to the occurrence of NPs. However, patients with CRS usually exhibit headaches, nasal congestion, and purulent nasal discharge, while symptoms of NPs are usually gradual nasal congestion, accompanied by decreased olfactory function [49]. In the future, more experiments are needed to further verify the CRS specificity of this study.
As widely described, lncRNA achieve its role in diseases by regulating downstream targets through binding with RBPs [50]. As proof, lncRNA XIST promoted osteoclast differentiation by increasing S1P expression through interacting with FUS [51]. Additionally, LINC01094 could facilitate gastric cancer proliferation and metastasis by upregulating through targeting AZGP1 [16]. Based on the above evidence, it can be preliminarily speculated that LINC01094 may play a role in CRSwNP by regulating downstream proteins through RBP. In the current study, it was found that LINC01094 promoted HMGB1 expression in CRSwNP by binding with RNA-binding protein FUS, which might be a potential mechanism by which LINC01094 regulated CRSwNP progression. HMGB1 is an important mediator of inflammation [52]. Notably, HMGB1 activation accelerated CRSwNP progression [20]. Herein, consistently, HMGB1 was significantly upregulated in nasal polyp tissues of CRSwNP patients, and hNEC isolated from tissues of CRSwNP patients and controls. Additionally, rhHMGB1 treatment reversed the inhibitory effects of LINC01094 downregulation on hNEC EMT and pyroptosis during CRSwNP progression. Collectively, LINC01094 promoted hNEC EMT and pyroptosis in CRSwNP by targeting HMGB1 through binding with FUS.
Snail functions in activating EMT by inhibiting E-cadherin [53]. Herein, Snail expression was markedly decreased in nasal polyp tissues of CRSwNP patients, and its expression was positively correlated with LINC01094 expression. However, the mechanism which regulates Snail is still unclear. It has been widely described that GSK-3β activation contributes to Snail nuclear import to induce EMT in GSK-3β phosphorylation-dependent manner [54, 55]. Our results revealed that HMGB1 promoted Snail nuclear import by inducing GSK-3β phosphorylation in CRSwNP patients-derived hNEC. As expected, Snail downregulation abrogated rhHMGB1's facilitation on hNEC EMT and pyroptosis. Therefore, we came to the conclusion that the GSK-3β/Snail pathway functioned as the downstream pathway of LINC01094/HMGB1 axis in promoting hNEC EMT and pyroptosis during CRSwNP progression. If conditions permit in the future, we will further validate our findings in vivo. Meanwhile, we will further investigate the proliferation mechanism of CRSwNP, which arouses our great interest.

Conclusion

Our research reported for the first time that the role of LINC01094 in promoting hNEC EMT and pyroptosis during CRSwNP progression, the underlying mechanism of which was promoting HMGB1 expression through binding with FUS to activate the GSK-3β/Snail pathway. The present study reveals that LINC01094 may be a potential therapeutic target for CRSwNP treatment.

Ethics approval and consent to participate

This study was passed the review of Ethics Committee of Hainan General Hospital, Hainan Affiliated Hospital of Hainan Medical University Hospital before enrollment of patients and all participants signed informed consent.

Consent for publication

The informed consent was obtained from study participants.

Availability of data and materials

The datasets generated during and/or analysed during the current study are available from the corresponding author on reasonable request.

Conflicts of interest

All authors agree with the presented findings, have contributed to the work, and declare no conflict of interest.

Funding

The authors express their gratitude to for his help for directing our article. This work was supported by grants from National Natural Science Foundation of China Regional Fund Program (82060184,81760187,82160210), Hainan Province Science and Technology Special Fund (ZDYF2022SHFZ049), Hainan Province Clinical Medical Center, Natural Science Research Project

"open competition mechanism" of Hainan Medical University (JBGS202109).

Authors' contributions

ZL: conceived the ideas; YF: designed the experiments; WH: performed the experiments; CL: analyzed the data; XW: provided critical materials; JBZ: wrote the manuscript; JZ: supervised the study. All the authors have read and approved the final version for publication.

Abbreviations

Chronic rhinosinusitis, (CRS); Chronic rhinosinusitis with nasal polyps, (CRSwNP); Epithelial-to-mesenchymal transition, (EMT); Nasal epithelial cells, (NECs); Long non-coding RNAs, (LncRNAs); Long intergenic non-coding RNA 01094, (LINC01094); High mobility group box-1, (HMGB1); Fused in sarcoma, (FUS); Glycogen synthase kinase, (GSK)-3β; Serine/threonine kinase, (AKT); 3-(4, 5-Dimethylthiazolyl2)-2, 5-diphenyltetrazolium bromide, (MTT); RNA immunoprecipitation, (RIP); Quantitative real-time polymerase chain reaction, (qRT-PCR); Standard deviation, (SD); Analysis of variance, (ANOVA).

References

1. Benjamin MR, Stevens WW, Li N, Bose S, Grammer LC, Kern RC, et al. Clinical characteristics of patients with chronic rhinosinusitis without nasal polyps in an academic setting. J Allergy Clin Immunol Pract. 2019;7(3):1010-6.
2. Bhattacharyya N, Villeneuve S, Joish VN, Amand C, Mannent L, Amin N, et al. Cost burden and resource utilization in patients with chronic rhinosinusitis and nasal polyps. Laryngoscope. 2019;129(9):1969-75.
3. Amedee RG. Prevalence of polyp recurrence after endoscopic sinus surgery for chronic rhinosinusitis with nasal polyposis. Am J Rhinol Allergy. 2017;31(4):278.
4. Jiang W, Zhou C, Ma C, Cao Y, Hu G, Li H. TGF-β1 induces epithelial-to-mesenchymal transition in chronic rhinosinusitis with nasal polyps through microRNA-182. Asian Pac J Allergy Immunol. 2021.
5. Li Y, Chang LH, Huang WQ, Bao HW, Li X, Chen XH, et al. IL-17A mediates pyroptosis via the ERK pathway and contributes to steroid resistance in CRSwNP. The Journal of allergy and clinical immunology. 2022;150(2):337-51.
6. Xia Y, Wang H, Yin J. The role of epithelial-mesenchymal transition in chronic rhinosinusitis. Int Arch Allergy Immunol. 2022;183(10):1029-39.
7. Yang N, Cheng H, Mo Q, Zhou X, Xie M. miR-155-5p downregulation inhibits epithelial-to-mesenchymal transition by targeting SIRT1 in human nasal epithelial cells. Mol Med Rep. 2020;22(5):3695-704.
8. Wu X, Yuan Y, Ma R, Xu B, Zhang R. lncRNA SNHG7 affects malignant tumor behaviors through downregulation of EZH2 in uveal melanoma cell lines. Oncol Lett. 2020;19(2):1505-15.
9. Wang X, Zhu X, Peng L, Zhao Y. Identification of lncRNA biomarkers and LINC01198 promotes progression of chronic rhinosinusitis with nasal polyps through sponge miR-6776-5p. Biomed Res Int. 2022;2022:9469207.
10. Xu J, Zhang P, Sun H, Liu Y. LINC01094/miR-577 axis regulates the progression of ovarian cancer. J Ovarian Res. 2020;13(1):122.
11. Li XX, Yu Q. Linc01094 Accelerates the Growth and metastatic-related traits of glioblastoma by sponging miR-126-5p. Onco Targets Ther. 2020;13:9917-28.
12. Ye Y, Ge O, Zang C, Yu L, Eucker J, Chen Y. LINC01094 Predicts poor prognosis in patients with gastric cancer and is correlated with EMT and macrophage infiltration. Technol Cancer Res Treat. 2022;21:15330338221080977.
13. Sun Q, Gao Y, Zhang Y, Cao H, Liu J, Neo SY, et al. Prognostic profiling of the EMT-associated and immunity-related lncrnas in lung squamous cell carcinomas. Cells. 2022;11(18).
14. Ferrè F, Colantoni A, Helmer-Citterich M. Revealing protein-lncRNA interaction. Briefings Bioinform. 2016;17(1):106-16.
15. Chen Q, Zhou L, Ma D, Hou J, Lin Y, Wu J, et al. LncRNA GAS6-AS1 facilitates tumorigenesis and metastasis of colorectal cancer by regulating TRIM14 through miR-370-3p/miR-1296-5p and FUS. J Transl Med. 2022;20(1):356.
16. Gong Z, Zhang Y, Yang Y, Yang Y, Zhang J, Wang Y, et al. LncRNA LINC01094 promotes cells proliferation and metastasis through the PTEN/AKT pathway by targeting AZGP1 in gastric cancer. Cancers (Basel). 2023;15(4).
17. Martinotti S, Patrone M, Ranzato E. Emerging roles for HMGB1 protein in immunity, inflammation, and cancer. Immunotargets Ther. 2015;4:101-9.
18. Zhu D, Zou H, Liu J, Wang J, Ma C, Yin J, et al. Inhibition of HMGB1 ameliorates the maternal-fetal interface destruction in unexplained recurrent spontaneous abortion by suppressing pyroptosis activation. Front Immunol. 2021;12:782792.
19. Chen D, Mao M, Bellussi LM, Passali D, Chen L. Increase of high mobility group box chromosomal protein 1 in eosinophilic chronic rhinosinusitis with nasal polyps. Int Forum Allergy Rhinol. 2014;4(6):453-62.
20. Chen D, Bellussi LM, Cocca S, Wang J, Passali GC, Hao X, et al. Glycyrrhetinic acid suppressed hmgb1 release by up-regulation of Sirt6 in nasal inflammation. J Biol Regul Homeost Agents. 2017;31(2):269-77.
21. Chang HY, Chen SY, Wu CH, Lu CC, Yen GC. Glycyrrhizin attenuates the process of epithelial-to-mesenchymal transition by modulating HMGB1 initiated novel signaling pathway in prostate cancer cells. J Agric Food Chem. 2019;67(12):3323-32.
22. Fokkens WJ, Lund VJ, Hopkins C, Hellings PW, Kern R, Reitsma S, et al. European position paper on rhinosinusitis and nasal polyps 2020. Rhinology. 2020;58(Suppl S29):1-464.
23. Abbas EE, Li C, Xie A, Lu S, Tang L, Liu Y, et al. Distinct clinical pathology and microbiota in chronic rhinosinusitis with nasal polyps endotypes. Laryngoscope. 2021;131(1):E34-e44.
24. Zhang XH, Zhang YN, Li HB, Hu CY, Wang N, Cao PP, et al. Overexpression of miR-125b, a novel regulator of innate immunity, in eosinophilic chronic rhinosinusitis with nasal polyps. Am J Resp Crit Care Med. 2012;185(2):140-51.
25. Wang H, Hu DQ, Xiao Q, Liu YB, Song J, Liang Y, et al. Defective STING expression potentiates IL-13 signaling in epithelial cells in eosinophilic chronic rhinosinusitis with nasal polyps. J Allergy Clin Immunol. 2021;147(5):1692-703.
26. Bae JS, Ryu G, Kim JH, Kim EH, Rhee YH, Chung YJ, et al. Effects of Wnt signaling on epithelial to mesenchymal transition in chronic rhinosinusitis with nasal polyp. Thorax. 2020;75(11):982-93.
27. Liu C, Du H, Wang Y, Gong N, Qi W, Zhou X, et al. S100A11 regulates nasal epithelial cell remodeling and inflammation in CRSwNPs via the RAGE-mediated AMPK-STAT3 pathway. Mol Immunol. 2021;140:35-46.
28. Matsunaga K, Katoh N, Fujieda S, Izuhara K, Oishi K. Dupilumab: Basic aspects and applications to allergic diseases. Allergol Int. 2020;69(2):187-96.
29. Li Z, Zeng M, Deng Y, Zhao J, Zhou X, Trudeau JB, et al. 15-Lipoxygenase 1 in nasal polyps promotes CCL26/eotaxin 3 expression through extracellular signal-regulated kinase activation. J Allergy Clin Immunol. 2019;144(5):1228-41.e9.
30. Wang Y, Wang X, Jin M, Lu J. Activation of the hedgehog signaling pathway is associated with the promotion of cell proliferation and epithelial-mesenchymal transition in chronic rhinosinusitis with nasal polyps. Eur Arch Otorhinolaryngol.

2023;280(3):1241-51.
31. Zhao H, Wang L, Wang S, Chen X, Liang M, Zhang X, et al. CHN1 promotes epithelial-mesenchymal transition via the Akt/GSK-3β/Snail pathway in cervical carcinoma. J Transl Med. 2021;19(1):295.
32. Kato A. Immunopathology of chronic rhinosinusitis. Allergol Int. 2015;64(2):121-30.
33. He Y, Meng XM, Huang C, Wu BM, Zhang L, Lv XW, et al. Long noncoding RNAs: novel insights into hepatocelluar carcinoma. Cancer Lett. 2014;344(1):20-7.
34. Liao K, Xu J, Yang W, You X, Zhong Q, Wang X. The research progress of LncRNA involved in the regulation of inflammatory diseases. Mol Immunol. 2018;101:182-8.
35. Chen H, Liu Y, Liu P, Dai Q, Wang P. LINC01094 promotes the invasion of ovarian cancer cells and regulates the Wnt/β-catenin signaling pathway by targeting miR-532-3p. Exp Ther Med. 2021;22(5):1228.
36. Fokkens WJ, Lund VJ, Mullol J, Bachert C, Alobid I, Baroody F, et al. EPOS 2012: European position paper on rhinosinusitis and nasal polyps 2012. A summary for otorhinolaryngologists. Rhinology. 2012;50(1):1-12.
37. Kook JH, Kim HJ, Kim KW, Park SJ, Kim TH, Lim SH, et al. The expression of 11β-hydroxysteroid dehydrogenase type 1 and 2 in nasal polyp-derived epithelial cells and its possible contribution to glucocorticoid activation in nasal polyp. Am J Rhinol Allergy. 2015;29(4):246-50.
38. Liao B, Cao PP, Zeng M, Zhen Z, Wang H, Zhang YN, et al. Interaction of thymic stromal lymphopoietin, IL-33, and their receptors in epithelial cells in eosinophilic chronic rhinosinusitis with nasal polyps. Allergy. 2015;70(9):1169-80.
39. Liu JX, Chen AN, Yu Q, Shi KT, Liu YB, Guo CL, et al. MEX3B inhibits collagen production in eosinophilic nasal polyps by downregulating epithelial cell TGFBR3 mRNA stability. JCI Insight. 2023;8(9).
40. Lambrecht BN, Hammad H, Fahy JV. The cytokines of asthma. Immunity. 2019;50(4):975-91.
41. Xu J, Lee JW, Park SK, Lee SB, Yoon YH, Yeon SH, et al. Toll-like receptor 9 ligands increase type I interferon induced B-cell activating factor expression in chronic rhinosinusitis with nasal polyposis. Clin Immunol. 2018;197:19-26.
42. Xu Z, Huang Y, Delemarre T, Cavaliere C, Zhang N, Bachert C. Advances in chronic rhinosinusitis in 2020 and 2021. J Allergy Clin Immunol. 2022;149(3):854-66.
43. Chen N, Chen CC, Lau LF. Adhesion of human skin fibroblasts to Cyr61 is mediated through integrin alpha 6beta 1 and cell surface heparan sulfate proteoglycans. J Biol Chem. 2000;275(32):24953-61.
44. Chen CC, Chen N, Lau LF. The angiogenic factors Cyr61 and connective tissue growth factor induce adhesive signaling in primary human skin fibroblasts. J Biol Chem. 2001;276(13):10443-52.
45. Deng H, Li M, Zheng R, Qiu H, Yuan T, Wang W, et al. YAP Promotes cell proliferation and epithelium-derived cytokine expression via NF-κB pathway in nasal polyps. J Asthma Allergy. 2021;14:839-50.
46. Bequignon E, Mangin D, Bécaud J, Pasquier J, Angely C, Bottier M, et al. Pathogenesis of chronic rhinosinusitis with nasal polyps: role of IL-6 in airway epithelial cell dysfunction. J Transl Med. 2020;18(1):136.
47. Fidler TP, Xue C, Yalcinkaya M, Hardaway B, Abramowicz S, Xiao T, et al. The AIM2 inflammasome exacerbates atherosclerosis in clonal haematopoiesis. Nature. 2021;592(7853):296-301.
48. Barekzi E, Roman J, Hise K, Georas S, Steinke JW. Lysophosphatidic acid stimulates inflammatory cascade in airway epithelial cells. Prostaglandins Leukot Essent Fatty Acids. 2006;74(6):357-63.
49. Ta NH. Will we ever cure nasal polyps? Ann R Coll Surg Engl. 2019;101(1):35-9.
50. Pereira B, Billaud M, Almeida R. RNA-Binding proteins in cancer: old players and new actors. trends cancer. 2017;3(7):506-28.
51. Zhang DW, Wang HG, Zhang KB, Guo YQ, Yang LJ, Lv H. LncRNA XIST facilitates S1P-mediated osteoclast differentiation via interacting with FUS. J Bone Miner Metab. 2022;40(2):240-50.
52. Chen G, Ward MF, Sama AE, Wang H. Extracellular HMGB1 as a proinflammatory cytokine. J Interferon Cytokine Res. 2004;24(6):329-33.
53. Becker KF, Rosivatz E, Blechschmidt K, Kremmer E, Sarbia M, Höfler H. Analysis of the E-cadherin repressor Snail in primary human cancers. Cells Tissues Organs. 2007;185(1-3):204-12.
54. Zhou BP, Deng J, Xia W, Xu J, Li YM, Gunduz M, et al. Dual regulation of Snail by GSK-3beta-mediated phosphorylation in control of epithelial-mesenchymal transition. Nat Cell Biol. 2004;6(10):931-40.
55. Liu Y, Zhou H, Zhu R, Ding F, Li Y, Cao X, et al. SPSB3 targets SNAIL for degradation in GSK-3β phosphorylation-dependent manner and regulates metastasis. Oncogene. 2018;37(6):768-76.

Jing Zheng
Department of Otorhinolaryngology
Head and Neck Surgery
Hainan General Hospital
Hainan Affiliated Hospital of Hainan
Medical University
No.19, Xiuhua Road
Xiuying District
Haikou 570311
Hainan Province
P.R. China

Tel:+86-0898-66772248
E-mail: serena_zheng@163.com

This manuscript contains online supplementary material

SUPPLEMENTARY MATERIAL

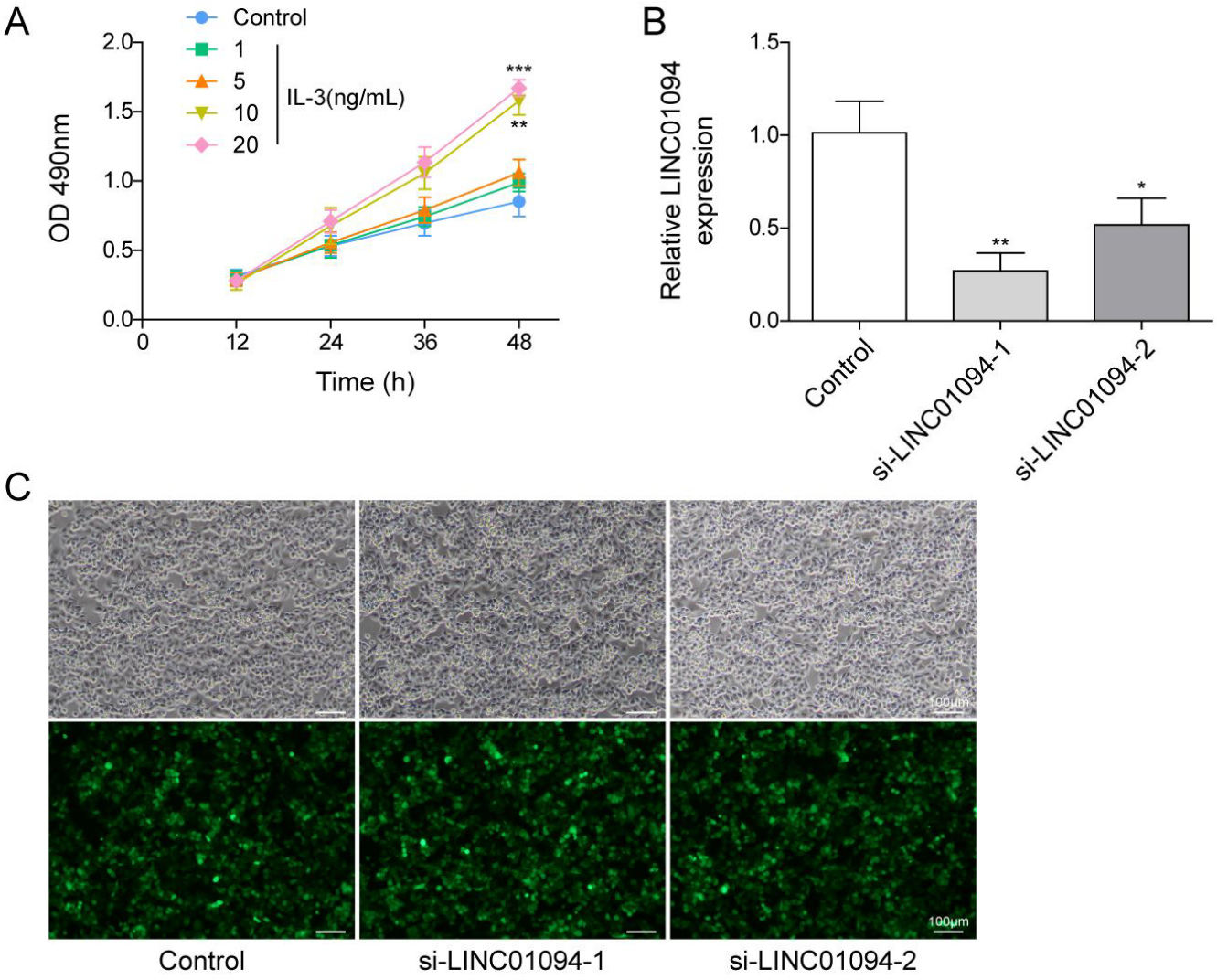

Figure S1. (A) hNECs were treated with different concentrations of IL-13 (1, 5, 10 and 20 ng/mL) for 12, 24, 36 and 48 h, and cell viability was examined by MTT assay. (B) LINC01094 expression in hNECs transfected with si-LINC01094-1, si-LINC01094-2 or si-NC was detected by qRT-PCR. (C) Fluorescence microscope observations of hNECs transfected with si-LINC01094-1, si-LINC01094-2 or si-NC were presented. The measurement data were presented as mean ± SD. All data was obtained from at least three replicate experiments. *p < 0.05, **p < 0.01, ***p < 0.001.

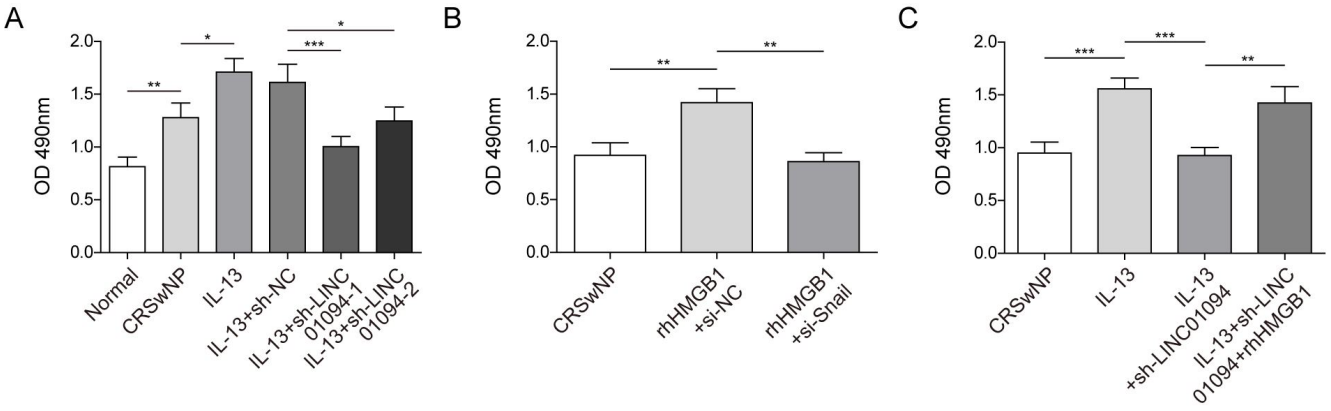

Figure S2. (A) CRSwNP patients-derived hNEC were transfected with si-NC or si-LINC01094 and subsequently subjected to IL-13 stimulation, and cell viability was examined by MTT assay. (B) CRSwNP patients-derived hNEC were treated with rhHMGB1 and transfected with si-Snail meanwhile, and cell viability was detected using MTT assay. (C) CRSwNP patients-derived hNEC were treated with rhHMGB1 and transfected with si-LINC01094 meanwhile, and cell viability was determined by MTT assay. The measurement data were presented as mean ± SD. All data was obtained from at least three replicate experiments. *p < 0.05, **p < 0.01, ***p < 0.001.

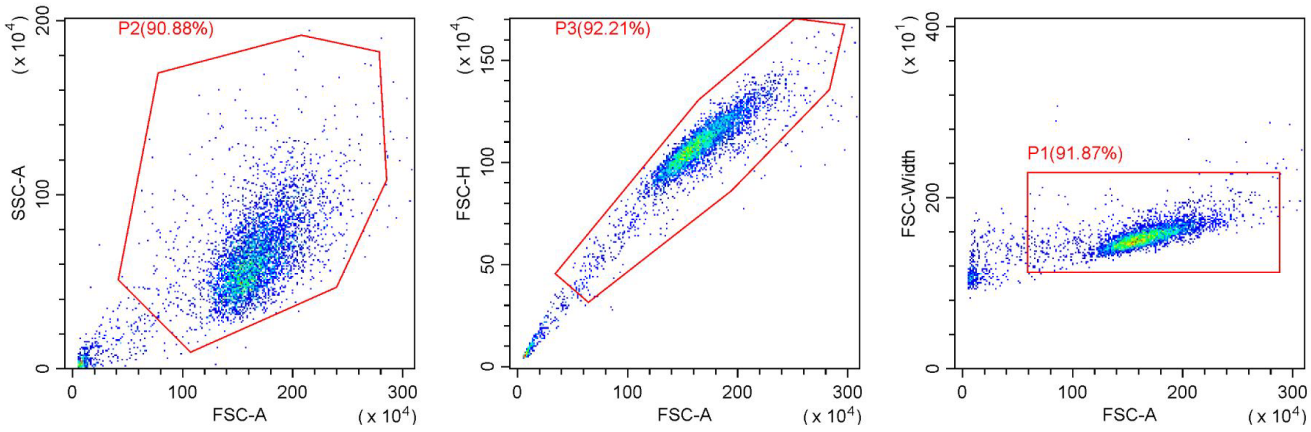

Figure S3. A gating strategy is shown (FSC vs SSC, Live/death marker and singlets). All data was obtained from at least three replicate experiments.